

Entanglement Witness Derived By Using Kolmogorov-Arnold Networks

1st Fatemeh Lajevardi¹, 2nd Azam Mani¹, 3rd Ali Fahim¹

¹*Department of Engineering Sciences, College of Engineering, University of Tehran, Tehran, Iran*

Emails: fatemeh.lajevardi@ut.ac.ir, mani.azam@ut.ac.ir, a.fahim@ut.ac.ir

Abstract—We utilize Kolmogorov-Arnold Networks to design an interpretable model capable of detecting quantum entanglement within a set of nine-parameter two-qubit states. This network serves as an entanglement witness, achieving an accuracy of 94% in distinguishing entangled states. Additionally, by analyzing the output functions of the KAN models, we explore the significance of each parameter (feature) in identifying the presence of entanglement. This analysis enables us to rank the features and eliminate the less significant ones, leading to the development of new entanglement witness functions that rely on fewer number of features, and hence do not require complete state tomography for their evaluation.

Index Terms—Entanglement, Separable, KAN, Witness, Observable

I. INTRODUCTION

Quantum entanglement is one of the most important features of quantum mechanics, underpinning many phenomena and technologies that distinguish quantum systems from their classical counterparts. It serves as a critical resource for quantum computation, quantum communication, and quantum cryptography, enabling applications such as quantum teleportation and super-dense coding [1]. Entanglement is in fact a type of quantum correlation that can exist in a composite system of at least two parts. The Quantum state of a composite system is entangled if it can not be prepared solely by local operations and classical communications (LOCC) of the parties involved. However, detecting and quantifying entanglement, especially in systems of increasing complexity, remain significant challenges in quantum information science [2], [3]. Entanglement witnesses, a class of Hermitian operators, provide a practical solution for identifying entangled states from the on-entangled ones (separable stats) [4]. By measuring the expectation value of a witness operator, one can determine whether a quantum state is entangled, i.e. a negative expectation value of an entanglement witness indicates the presence of entanglement. It is also challenging to define an appropriate witness operator to ensure positive results for separable states and negative results for most entangled states, that is why many researches have been done to design practically measurable entanglement witnesses for different system sizes [5], [6]. For example, for two-qubit systems, the positivity of the partial transpose (PPT) of the density matrix serves as a witness function [7], although it still requires complete tomography of the state.

Recently, the widespread adoption of machine learning and deep learning, along with their effective solutions, has led many researchers to embrace these methods for addressing the entanglement witness issue. For example, some entanglement witnesses are offered based on the SVM techniques, for two- and three-qubit systems [8]–[10].

Kolmogorov-Arnold Networks (KANs) are a class of recently introduced neural networks which offer innovative alternatives to traditional multi-layer perceptrons (MLPs) in the field of neural networks [11]. The backbone of this network is based on the Kolmogorov-Arnold theorem, which states that for a multivariate continuous function on a bounded domain, it is possible to construct the function, by using a summation of continuous functions of single variables. This result can be explained by the following equation [12].

$$f(x) = f(x_1, \dots, x_n) = \sum_{q=1}^{2n+1} \Phi_q \left(\sum_{p=1}^n \phi_{q,p}(x_p) \right) \quad (1)$$

where:

- $f : [0, 1]^n \rightarrow \mathbb{R}$
- $\phi_{q,p} : [0, 1] \rightarrow \mathbb{R}$ are continuous functions of single a variable,
- $\Phi_q : \mathbb{R} \rightarrow \mathbb{R}$ are continuous functions.

This network is designed to learn the univariate functions $\phi_{q,p}$ and Φ_q instead of directly learning the multivariate function f . This decomposition reduces the complexity of the problem, as learning univariate functions is often easier than learning multivariate ones. Unlike MLPs, which use fixed activation functions assigned to individual neurons, KANs employ learnable activation functions applied to the edges or weights of the network, replacing conventional linear weight matrices with spline functions [11]. Figure 1 illustrates the schematic structure of such networks. The unique architecture of KAN facilitates the effective summation of incoming signals while avoiding typical nonlinearities, potentially resulting in more compact computation graphs compared to their MLP counterparts. KANs harness the complementary strengths of both MLPs and splines: MLPs excel at learning compositional structures, while splines are adept at accurately approximating low-dimensional functions. Consequently, KANs effectively mitigate the curse of dimensionality associated with spline methods, enhancing both accuracy and interpretability across

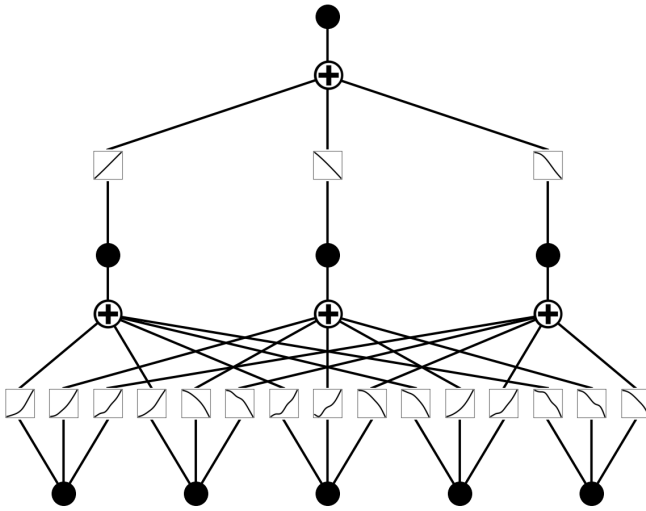


Fig. 1. The schematic structure of a Kolmogorov-Arnold Neural Network (KAN): This sample model consists of an input layer with 5 nodes, a single hidden layer containing 3 nodes, and an output layer with 1 node. As illustrated, each edge in the network is associated with an activation function that must be optimized during the learning process. The outputs of these activation functions are summed before being passed to the nodes of the subsequent layer.

various applications, particularly in scientific domains. Empirical evaluations demonstrate that KANs consistently outperform MLPs, especially in small-scale artificial intelligence and scientific tasks [13].

Interpretability of the results provided by Kolmogorov-Arnold Networks, motivated us to introduce a novel method for detecting entanglement of two-qubit states by utilizing these Networks. Rooted in the Kolmogorov-Arnold representation theorem, KANs offer a robust framework for approximating functions while maintaining interpretability and accuracy. Our research focuses on two-qubit systems, and we construct a dataset of quantum states that spans both entangled and separable regions, ensuring uniform distribution across the data space. By training KAN models on this dataset, we demonstrate their capability to classify quantum states with high accuracy. Additionally, by utilizing the output functions of the KAN network, we derive some entanglement witnesses that do not necessitate complete state tomography for the evaluation of their expectation values, in other words, we reduce the required features. There are also other studies that have developed simple networks to reduce the number of measurements needed for entanglement detection [14]. However, it is important to note that the derived measurements from these methods are not locally applicable. While we decrease the number of required features, which directly leads to a reduction in the number of necessary local measurements. On the other hand, we highlight that many studies examining the entanglement properties of two-qubit systems within the framework of machine learning typically focus on the one-parameter family

of Werner states to construct their entangled datasets. In contrast, our research expands this scope by considering a nine-parameter family of both entangled and separable two-qubit states for our dataset, significantly broadening the range compared to previous investigations [9], [10].

The paper is structured as follows: In section II we briefly review the feature space of two qubit states and describe the structure of our data set. Section III details the architecture and training process of the KAN models, and section IV discusses the extraction of entanglement witnesses and their validation. Finally, Section IV presents the conclusions and potential avenues for future research.

II. TWO-QUBIT SYSTEMS

Any two-qubit state, represented by a 4×4 density matrix, can be expanded in terms of Pauli matrices

$$\rho = \frac{1}{4} \left[I \otimes I + \sum_{i=1}^3 a_i \sigma_i \otimes I + b_i I \otimes \sigma_i + \sum_{i,j=1}^3 t_{ij} \sigma_i \otimes \sigma_j \right], \quad (2)$$

where \otimes represents the tensor product, σ_i , $i = \{1, 2, 3\}$ stands for the Pauli matrices, a_i , b_i and t_{ij} are real coefficients. Hence, any arbitrary two qubit state has 15 independent features, that physically are the expectation values of the Pauli matrices and can be extracted by Pauli matrix measurements. For example, t_{ij} is the expectation value of $\sigma_i \otimes \sigma_j$, i.e. $t_{ij} = \text{Tr}(\rho \sigma_i \otimes \sigma_j)$, and it can be obtained by measuring the hermitian observable $\sigma_i \otimes \sigma_j$. Using representation (2) facilitates the future definition of entanglement witnesses that should be hermitian observables. We note that, while the Pauli matrices are traditionally denoted as σ_1 , σ_2 , and σ_3 , it is sometimes more convenient and clearer to adopt the notation X , Y , and Z for these matrices, respectively. Accordingly, we will use the symbols XX and XY in place of $\sigma_1 \otimes \sigma_1$ and $\sigma_1 \otimes \sigma_2$, respectively, applying similar compact notation for the other combinations. This notation will be used more throughout the section IV.

Here, we only consider two-qubit states with maximally mixed marginals, i.e. $a_i = b_i = 0$, for $i = \{1, 2, 3\}$. To generate such states, one can randomly generate sets of the coefficients t_{ij} and only keeps the sets that ensure the positivity of density matrix (2). This approach is not only inefficient, but it also fails to yield a uniform distribution of density matrices as obtained through Haar measure.

An alternative approach involves beginning with locally rotated versions of our target states, specifically the states referred to as *X-states*. Once we generate random X-states, we can obtain arbitrary states with maximally mixed marginals by applying random local unitaries to these X-states. A general X-state can be written as

$$\rho_X = \frac{1}{4} \left(I \otimes I + \sum_{k=1}^3 t_k \sigma_k \otimes \sigma_k \right), \quad (3)$$

which has non-zero values only along the diagonal and off-diagonal elements, while representing in the computational basis. The positivity of the density matrix (3), restricts the coefficients t_1 , t_2 , and t_3 to lie in a tetrahedron defined by the following equations

$$\begin{aligned} 1 - t_1 - t_2 - t_3 &\geq 0, \\ 1 - t_1 + t_2 + t_3 &\geq 0, \\ 1 + t_1 - t_2 + t_3 &\geq 0, \\ 1 + t_1 + t_2 - t_3 &\geq 0. \end{aligned} \quad (4)$$

As mentioned above, to ensure the creation of randomly distributed two-qubit states with maximally mixed marginals, we must undertake two key actions. First, we need to generate uniform samples of X-states. Second, we should apply a collection of appropriately uniformly distributed unitary matrices, to locally rotate these X-states. It is important to note that since local unitary operators do not alter the physical properties of the systems, the source and target classes of states (Entangled or Separable) remain invariant, while their domain expands across the two-qubit state space. For the first step, we randomly generate the point (t_1, t_2, t_3) within the constraints $-1 \leq t_1, t_2, t_3 \leq 1$, and we include it in the X-state dataset if it satisfies equation (4). For the second step, we generate random unitary operators U_1 and U_2 with accord to the Harr measure, and we add the following states to the data set

$$\rho = (U_1 \otimes U_2) \rho_x (U_1^\dagger \otimes U_2^\dagger). \quad (5)$$

Uniformity of the states ρ_x , and the operators U_1 and U_2 warrants the uniformity of our data set. The states (5) were then rewritten in the form (2), to obtain nine independent features t_{ij} .

We finally used the PPT criterion to determine the class of each X-state (the label associated to each X-state). Once the labels of X-states are determined, the labels of other states will automatically be obtained, since the local unitary operators do not change the label of states.

In addition to the above dataset, we have also considered a family of symmetric states as an extra dataset. These states are invariant under local unitary rotations around the z-axis, i.e.

$$(U \otimes U) \rho (U^\dagger \otimes U^\dagger) = \rho, \quad U = e^{i\theta\sigma_z}, \quad (6)$$

where θ is an arbitrary real parameter. The above condition reduces the number of no-zero features from nine to five. The Positive Partial Transpose (PPT) criterion has also been utilized for labeling this set.

III. MODEL STRUCTURE

The desired network for processing the generated dataset is KAN. To design a model using KAN, the PyKan library, which is available on GitHub, was employed [15]. In this research, two models were generated, based on the type of our dataset. Each model utilized a dataset consisting of 100,000 rows, 70% of which was used for training, 20%

for validation, and 10% for testing to assess the model's accuracy. Half of the dataset consists of separable states, while the other half comprises entangled states.

The initial models are as follows: For the first dataset, we used a model with an architecture comprising two hidden layers with sizes 6 and 3, respectively, an input layer of size 9, and an output layer of size 1. For the second dataset, we developed a model with only one hidden layer of size 3, an input layer of size 5 and an output layer of size 1. The number of the hidden layers and the size of each layer were considered as hyperparameters of the model and determined in the validation stage beside the other model's parameters.

To investigate the robustness of our models against the noise, we add some noise to the datasets in order to help the models adapt to noisy data (noisy measurement results). This noise was generated according to a Gaussian distribution with 0 mean and a standard deviation of 0.1. Considering this noise, the accuracy of both models were reduced to the reliable values 90%, from 94% and 0.98%.

TABLE I
CLASSIFICATION REPORT MODEL 9-6-3-1

	precision	recall	f1-score
Separable	0.95	0.94	0.94
Entanglement	0.94	0.95	0.94
accuracy			0.94

TABLE II
CLASSIFICATION REPORT MODEL 5-3-1

	precision	recall	f1-score
Separable	0.96	1.00	0.98
Entanglement	1.00	0.96	0.98
accuracy			0.98

IV. EXTRACTING WITNESS FROM MODEL

The defining characteristic of the Kolmogorov-Arnold Network that captures our attention is its capability to elucidate the model's final output as a function of the input features. In the context of the entanglement decision problem, a KAN generates a function that takes the initial features as inputs and produces an output value ranging from 0 to 1. If this output value is less than 0.5, the input state is classified as separable; otherwise, the state is categorized as entangled. Notably, this output function serves as an entanglement witness. For the models discussed in the previous section, the input features encompass all parameters of the density matrix, necessitating complete state tomography to determine the function's output. In this section, we only consider our general data set with nine features, and we analyze the output function to identify the most significant features relevant to the entanglement decision task. Our goal is to construct entanglement witness functions that utilize fewer features, thereby eliminating the need for complete state tomography. It's worth noting that our approach can also be utilized in

the symmetric dataset, but we've left out that analysis for the sake of brevity.

Before proceeding, we need to clarify the notation that will be used for the remainder of the paper. As previously mentioned, our dataset consists of a family of quantum states characterized by nine features t_{ij} , where $i, j \in \{1, 2, 3\}$. Considering the expansion

$$\rho = \frac{1}{4} \left[I \otimes I + \sum_{i,j=1}^3 t_{ij} \sigma_i \otimes \sigma_j \right], \quad (7)$$

the t_{ij} coefficients represent the expectation values of the Pauli observables $\sigma_i \otimes \sigma_j$. For example t_{11} (t_{23}) is the expectation value of the operator $\sigma_1 \otimes \sigma_1$ ($\sigma_2 \otimes \sigma_3$), or by using the more convenient notation explained after equation (2), t_{11} (t_{23}) is the expectation value of the operator XX (YZ). Accordingly, when we talk about the importance of XX (YZ) in the upcoming figures and tables, we are referring to the importance of the feature t_{11} (t_{23}) that can be obtained from the XX (YZ) measurement results. Similar conventions are also used for other features. Fixing this notation, we are now ready to present our method for constructing entanglement witness functions by using fewer features.

After running our KAN model for a dataset of 100,000 density matrices, we analyzed the importance of each feature in the value of the output function. The output function is composed of a combination of sinusoidal and linear functions of features equation (8) shows a sample of such function. Although the PyKan library provides options to select various functions for model explanations, we opted for these two in order to more effectively assess feature importance. Figure 2 represents this analysis for the exported function. It is evident from the figure that the feature ZX has the minimal impact on the classification of the states, while the features XZ , YZ , and ZZ are identified as the most influential features in this specific model.

However, this analysis pertains to a single model, when multiple models are trained and their respective functions are analyzed, the conclusions may differ. To obtain more robust and reliable results, it is necessary to aggregate analyses across many models. To achieve this, we use a bootstrap method: we generate multiple independent datasets, apply a KAN model to each dataset, perform an analysis similar to that shown in Figure (2) for each model, and then combine the results from all these models. Finally, we use a specific procedure (explained below) to assess the importance of each feature. Our analysis shows that considering 20 independent datasets of 100,000 density matrices and evaluating the 20 output functions from these models can yield robust and reliable results.

After training 20 models, in order to sort the features according to their importance in the output functions, for each

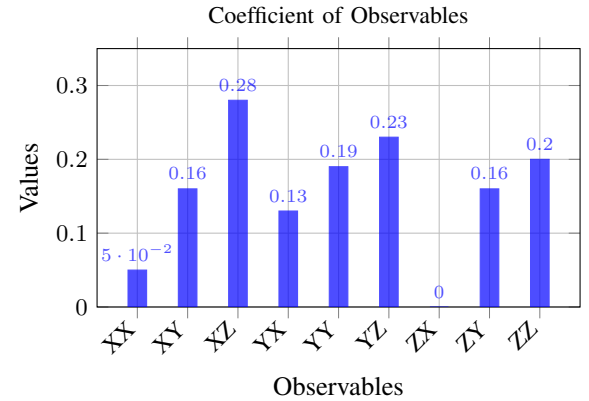


Fig. 2. The coefficients of observables for a sample output function from the model 9-6-3-1 are displayed, with the y-axis representing the coefficient values of the corresponding features on the x-axis.

model, we define eight groups for the features; namely Top-1, Top-2, ..., and Top-8. Top-1 contains the most important feature of the model, Top-2 contains the two most important features, and finally Top-8 contains all features except the less important one. We indicated the members of each group, for each model, and we then combined these individual results in Figure 3. The Figure shows each group by a line, and also illustrates the number of repetition of any feature as a members of each group. As a result, if we want to construct an entanglement witness, which depends only on four features (for example), then we should go to the Top-4 group, and select the four observables with the highest frequency of occurrence. We then construct a KAN model that works only with these four inputs. The output function of this KAN model will serve as an entanglement witness function. Table III summarizes the models that can be constructed by the results obtained from Figure 3.

TABLE III
VARIOUS DEGREES OF FEATURE REDUCTION, ALONG WITH THEIR ASSOCIATED OBSERVABLES AND MODEL STRUCTURE. EACH OBSERVABLE WAS SELECTED BASED ON ITS HIGHEST FREQUENCY OF APPEARANCE IN FIGURE3.

#Measurements	Observables	Model
1	YY	1-3-1
2	XZ, YY	2-3-1
3	XZ, YX, YY	3-2-1
4	XY, XZ, YX, YY	4-2-1
5	XX, XY, XZ, YX, YY	5-3-1
6	XX, XY, XZ, YX, YY, YZ	6-3-1
7	XX, XY, XZ, YX, YY, YZ, ZZ	7-5-3-1
8	XX, XY, XZ, YX, YY, YZ, ZX, ZY	8-5-3-1

This approach helps us to construct entanglement witness functions that depend on arbitrary number of observables. However, it should be noted that reducing the number of observables also decreases the accuracy of the witnesses.

Figure 4 illustrates the model's accuracy for different levels of feature reduction. This chart illustrates that using only four features (four observable measurements) enables us to classify states with over 80% of accuracy. Since four measurements provide us with a satisfactory accuracy, bellow we will present the witness function that we have obtained from our 4 – 2 – 1 model. Needless to say, this method is applicable to all proposed groups of observables presented in Figure 3.

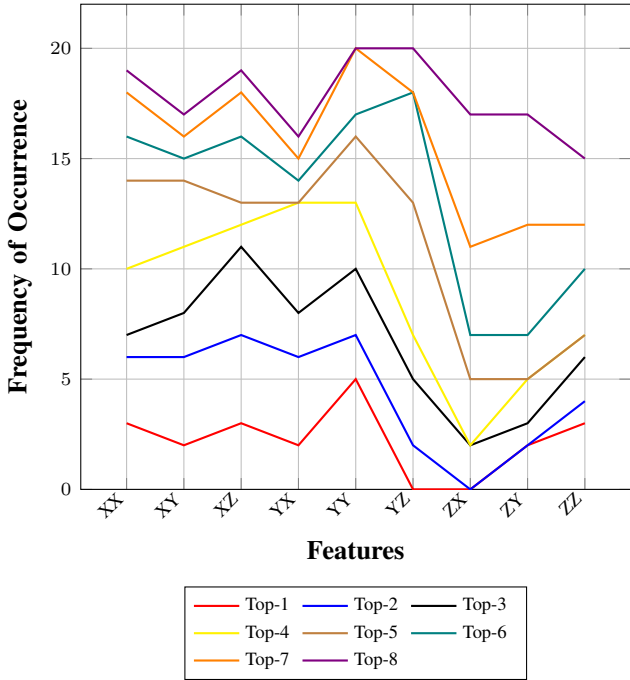


Fig. 3. Display the importance of observables in each group, where each line represents a group. For observables on the X-axis, the Y-axis indicates their frequency of occurrence within that group. For example, if a witness requires three observables, refer to the 'Top 3' line and select the three observables with the highest frequencies indicated on the Y-axis.

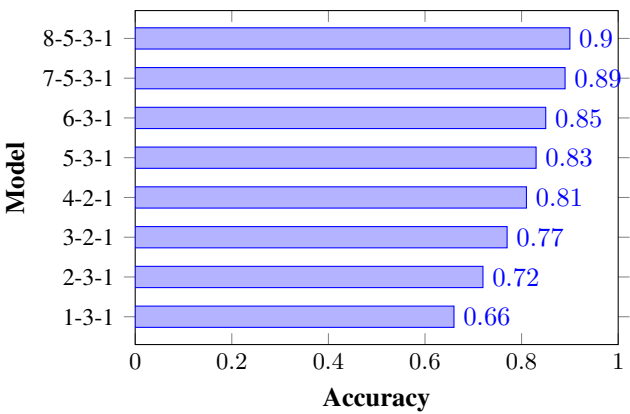


Fig. 4. Accuracy of each models with different number of reduced feature. All potential size of features, ranging from 1 to 8, are inserted.

For the four observables YX , YY , XZ , and XY , the extraction function phase concluded after training the model with these features. Subsequently, the `auto_symbolic` func-

tion from the PyKan library was used to fit a curve to the output generated by KAN. This function proposed sinusoidal and linear combinations of observables as witness functions. Equation (8) shows a sample witness function for this model. To simplify the witness and improve the readability, coefficients are rounded to two decimal places. It is valuable to note that one can obtain other equivalently important groups of observables and hence entanglement witnesses by cyclic permutations of Pauli matrices $X - Y - Z$.

$$\begin{aligned}
 W = & -0.12 \sin(5.49YX + 1.61) - 0.08 \sin(4.27YX - 7.79) \\
 & + 0.17 \sin(3.15XY - 1.58) - 0.15 \sin(4.43XY - 1.6) \\
 & + 0.14 \sin(5.02XZ - 1.57) - 0.06 \sin(4.41XZ + 1.6) \\
 & + 0.18 \sin(4.24YY - 1.59) + 0.22 \sin(2.65YY - 1.57) \\
 & + 1.88
 \end{aligned} \tag{8}$$

DISCUSSION

The results of this research demonstrate the potential of Kolmogorov-Arnold Networks (KANs) in the development of quantum entanglement witnesses for two-qubit systems. By leveraging the interpretability and flexibility of KANs, we successfully identified entanglement with a high degree of accuracy, using minimal measurement resources. Traditional methods for detecting entanglement often require complete state tomography or non-local measurements, which are resource-intensive. By contrast, the KAN-based approach presented in this study reduces the number of required measurements while maintaining high accuracy. This feature is particularly advantageous in experimental quantum setups, where measurement costs and noise can pose significant challenges. When comparing our KAN model with deep learning models such as [14], [16], [17], there may be no significant advantage in accuracy, as these models achieve near-perfect performance. However, in contrast to our model, their complex and non-descriptive nature makes it impossible to extract entanglement witnesses. On the other hand, SVM-based methods are more interpretable, allowing for witness extraction, but the key consideration of these models (compared to ours) is the restricted family of entangled states analyzed [8]–[10]. For example, [10] focuses only on the Werner states, and [9] examines just a subset of this family, achieving nearly 100% accuracy for these specific families. However, [8], which evaluates all entangled states, achieves 92% accuracy, lower than the 94% accuracy of our proposed method. In summary, the proposed method seeks to integrate the strengths of different approaches, but this comes at the cost of not delivering perfect accuracy across all cases.

While the proposed method shows significant promise, it is currently restricted to two-qubit systems. Extending the approach to multi-qubit and higher-dimensional systems, is the goal of our future research. As system size increases, the complexity of the entanglement structure grows exponentially, potentially requiring modifications to the KAN architecture or optimization techniques.

AI USAGE STATEMENT

The authors declare that they used artificial intelligence tools only to improve and edit the text of the article.

REFERENCES

- [1] M. A. Nielsen and I. L. Chuang, *Quantum Computation and Quantum Information*, Cambridge University Press, Dec 2010.
- [2] V. Vedral, M. B. Plenio, M. A. Rippin, and P. L. Knight "Quantifying Entanglement," *Physical Review Letters*, vol. 78, Mar 1997.
- [3] S. Gharibian "Strong NP-Hardness of the Quantum Separability Problem," *Quantum Information and Computation*, vol. 10, pp. 343-360, 2010.
- [4] O. Gühne and G. Tóth, "Entanglement Detection," *Physics Reports*, vol. 474, pp. 1–75, April 2009.
- [5] M. Horodecki, P. Horodecki, R. Horodecki, and K. Horodecki, "Separability of Mixed States: Necessary and Sufficient Conditions," *Physics Letters A*, vol. 223, pp. 1–8, Nov 1996.
- [6] Mohamed Bourennane, Manfred Eibl, Christian Kurtsiefer, Sascha Gaertner, Harald Weinfurter, Otfried Guehne, Philipp Hyllus, Dagmar Bruss, Maciej Lewenstein and Anna Sanpera, "Witnessing multipartite entanglement," *Physical Review Letters*, vol. 92, 2004.
- [7] Asher Peres, "Separability Criterion for Density Matrices," *Physical Review Letters*, vol. 77, Aug 1996.
- [8] Claudio Sanavio, Edoardo Tignone, and Elisa Ercolessi "Entanglement Classification via Witness Operators generated by Support Vector Machine," *The European Physical Journal - Plus*, vol. 138, October 2023.
- [9] Alexander C.B. Greenwood, Larry T.H. Wu, Eric Y. Zhu, Brian T. Kirby and Li Qian "Machine-Learning-Derived Entanglement Witnesses," *Physical Review Applied*, vol. 19, March 2023.
- [10] Mahmoud Mahdian and Zahra Mousavi "Optimal entanglement witness of multipartite systems using support vector machine approach," *Research Square*, July 2024.
- [11] Ziming Liu, Yixuan Wang, Sachin Vaidya, Fabian Ruehle, James Halverson, Marin Šoljačić, Thomas Y. Hou and Max Tegmark "KAN: Kolmogorov-Arnold Networks," *ICLR 2025 Conference*, Des 2024.
- [12] A. N. Kolmogorov "On the representation of continuous functions of many variables by superposition of continuous functions of one variable and addition," *Dokl. Akad. Nauk SSSR*, vol. 114, 1957.
- [13] Farhad Pourkamali-Anaraki "Kolmogorov-Arnold Networks in Low-Data Regimes: A Comparative Study with Multilayer Perceptrons," *ArXiv*, <https://arxiv.org/abs/2406.19738> Sep 2024.
- [14] Mohammad Yosefpor, Mohammad Reza Mostaan, and Sadegh Raeisi "Finding semi-optimal measurements for entanglement detection using Autoencoder Neural Networks," *Quantum Science and Technology*, Jul 2020.
- [15] Ziming Liu and collaborators, "Github," <https://github.com/KindXiaoming/pykan>, Des 2024.
- [16] Yiwei Chen, Yu Pan, Guofeng Zhang and Shuming Cheng "Detecting quantum entanglement with unsupervised learning," *Quantum Science and Technology*, vol. 7, 2021.
- [17] Naema Asif, Uman Khalid, Awais Khan, Trung Q. Duong and Hyundong Shin "Entanglement detection with artificial neural networks," *Scientific Reports*, vol. 13, 2024.